

# Implementation and Evaluation of WSR-88D Radial Velocity Data Assimilation for WRF-NMM via GSI

Shun Liu<sup>1</sup> and Ming Xue<sup>1,2</sup>,

<sup>1</sup>Center for Analysis and Prediction of Storms and <sup>2</sup>School of Meteorology  
University of Oklahoma, Norman OK 73019

## 1. Introduction

Weather Doppler radar has the capability to scan large volumes of the atmosphere at high spatial and temporal resolutions. The real time access to the data from the entire WSR-88D network became available in NCEP, which provides an unprecedented opportunity for using the data in operational numerical weather prediction (NWP) models. However, because of radar data quality problems and the huge volumes of radar data, how to use radar data properly in the current operational data assimilation system need to be investigated. During Shun Liu's visiting in EMC/NCEP supported by DTC and following-up one year, his work focused on improving and implementing radar radial velocity data quality control in NCEP real time data flow and testing the impact of radial wind on GSI analysis and WRF-NMM forecast.

## 2. Radar radial velocity quality control

Radar velocity quality control (QC) package has been developed by NSSL (Xu et al. 2004; Liu et al. 2003; Gong et al. 2004; Zhang et al. 2005 and Liu et al. 2005) for NCEP operational application. The QC package contains 4 parts: (1) radial velocity dealiasing, (2) ground clutter removal, (3) migrating bird detection and (4) noisy data removal.

Since 2005, NCEP has capability to real-time access to the level II data from any of the 120 National Weather Service (NWS) WSR-88D radars. All radar data from 120 radars are processed by 1 node/8 CPUs in operational IBM machine. Computation efficiency is very important for operational processing radar data. When Level II radar become available in NCEP, radar data is first uncompressed and decoding and then is converted into NCEP BUFR tank. Shun Liu has integrated Radar velocity QC package into radar raw data decoding part by redesigning and modifying the interface of NSSL QC package. Testing experiments were completed under operational computation environments in NCEP. The results showed that the original QC package took too much computation resource so that the radar data can not be real-time processed when QC package is used. Based on the needs of NCEP, the code structure of QC package is

further optimized and simplified. Before code optimization, the average time of processing a volume radar data is 25.6 s and it is 9.8 s after optimization. Other modification and improvements of QC package are listed in the below.

- Bug fix that QC package get the correct standard deviation on each tilt.
- Modify to use criterions of QC parameters depend on elevation angle.
- Estimate and specify the criterions of QC parameters for radar data volume scans with new VCP mode 121.
- Simplify bird migration algorithm and add it to QC package.
- Modify to allow that VAD wind can be used as a QC parameter.

## 3. Impact of radar radial wind on GSI analysis

Due to the high spatial and temporal resolution of radar wind, the amount of radar data is huge, which make it impossible to assimilate all of radar observations into operational system. Also the relatively low resolutions of the current operational models make the assimilation of full-volume data unnecessary. The fact that the definition of the radial velocity changes with the position of data relative to the radar poses an additional challenge not present with most other types of data; special treatment is therefore needed.

The super-obbing technique is developed by Purser et al. (2000) to reduce redundant information in the observational data as well as the data density. A "super-obbing" technique is used to preprocess the Level-II WSR-88D radar data (Parrish 2005) for thinning and combining radar radial velocity data. The "super-obbed" data are then analyzed in the NCEP unified GSI (Grid-point Statistical Interpolation) analysis system.

The impact of the super-obbed data on the analysis and WRF-NMM forecast are examined based on a mesoscale precipitation case. Two sets of experiments are designed. The first set of experiments is to examine the impact of background error decorrelation length,

while the second one is to examine the impact of the super-obs resolutions.

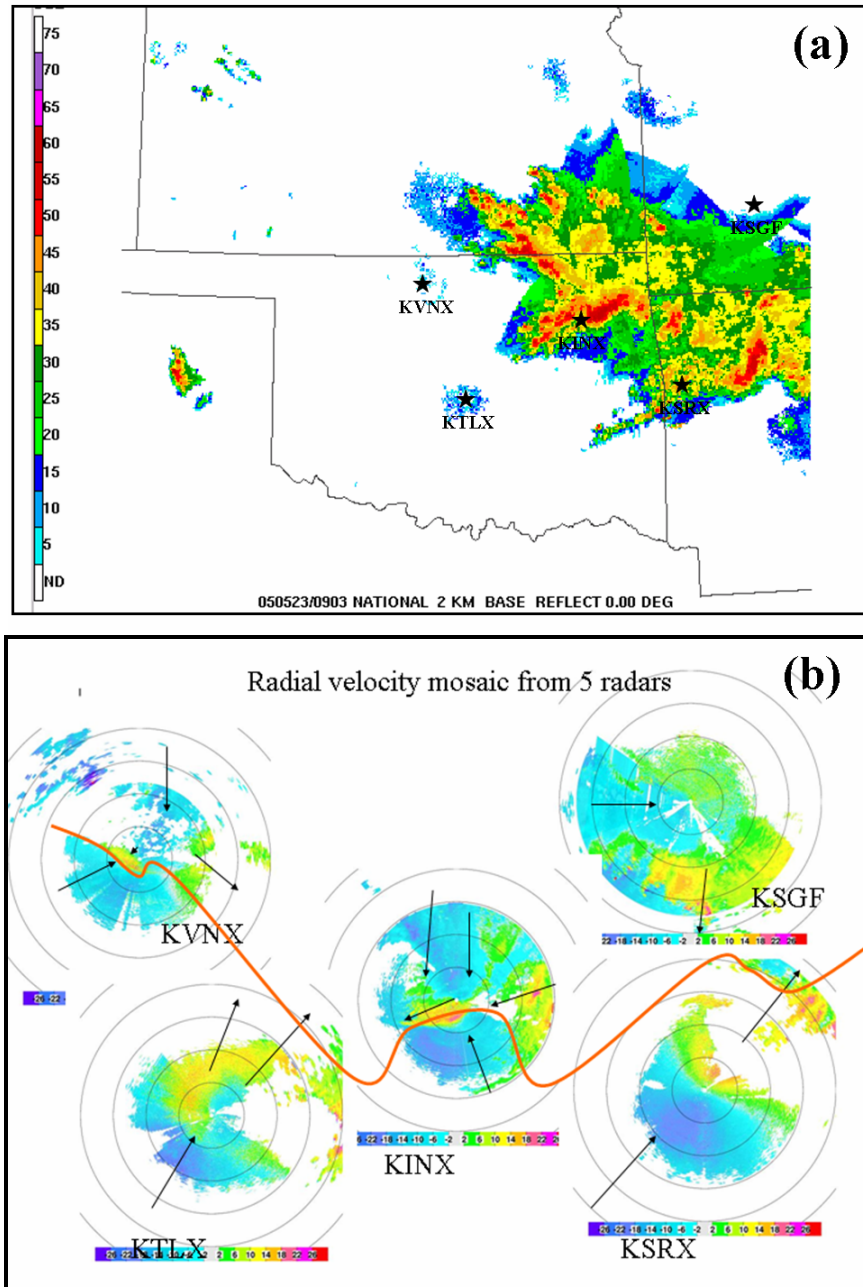


**Fig. 1.** The mosaiced radar reflectivity field at 0900 UTC on 23 May 2005 (a) and a crude mosaic of radial velocity (b) from the five radars marked in (a).

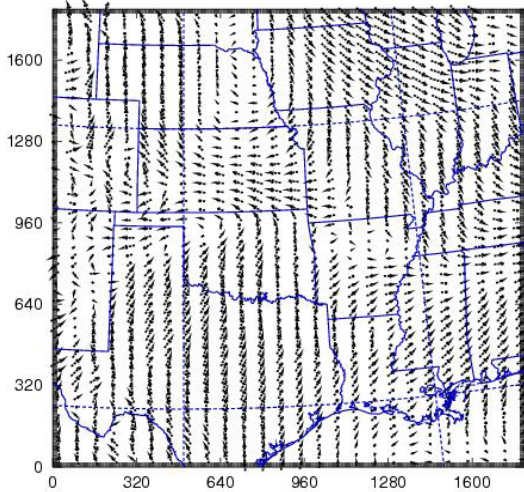


**Fig. 2.** The experimental WRF-NMM analysis of near surface winds at 0900 UTC on 23 May 2005 that is used as the analysis background in this study.

*a. Precipitation case of 23 May 2005*

Radar radial velocity data collected by the five radars located in Oklahoma, Kansas and Missouri, on 23 May 2005 are used to examine the impact of radial velocity on GSI wind field analysis. On that day, two convective cells formed near 0300 UTC near the Kansas-Oklahoma boundary, along a frontal zone. It developed into a mesoscale convective system with precipitation near 0900 UTC. This precipitation system was observed by five WSR-88D radars: KTLX, KINX, KSRX, KSGF and KVNK. The radar locations and reflectivity mosaic at 0900 UTC is shown in Fig. 1a. The maximum of radar reflectivity reaches 60 dBZ. A crude mosaic of radial velocity from five radars is shown in Fig. 1b.

A wind shift-line in Fig. 1b is marked by a yellow curved line. Northerly winds dominate north of the wind shift line, while southwesterly winds dominate to the south. The precipitation region is mainly located mid-east of the analysis domain.

The 8 km resolution 0900 UTC WRF-NMM analyzed wind using GSI without radar data is shown in Fig. 2. There exists a wind shift line near the northern boundary of Oklahoma in the analysis. The location of this wind shift line is too far north compared to the location indicated by the radar observations. The dominant wind direction is southwesterly south of the wind shift line and is easterly on the north side. Convergence is weak along this line in the analysis.

To examine the impact of radar radial wind data on the GSI analysis, two sets of experiments are designed. The first set of experiments is to examine the impact of background error decorrelation length, while the

second one is to examine the impact of the super-obs resolutions.

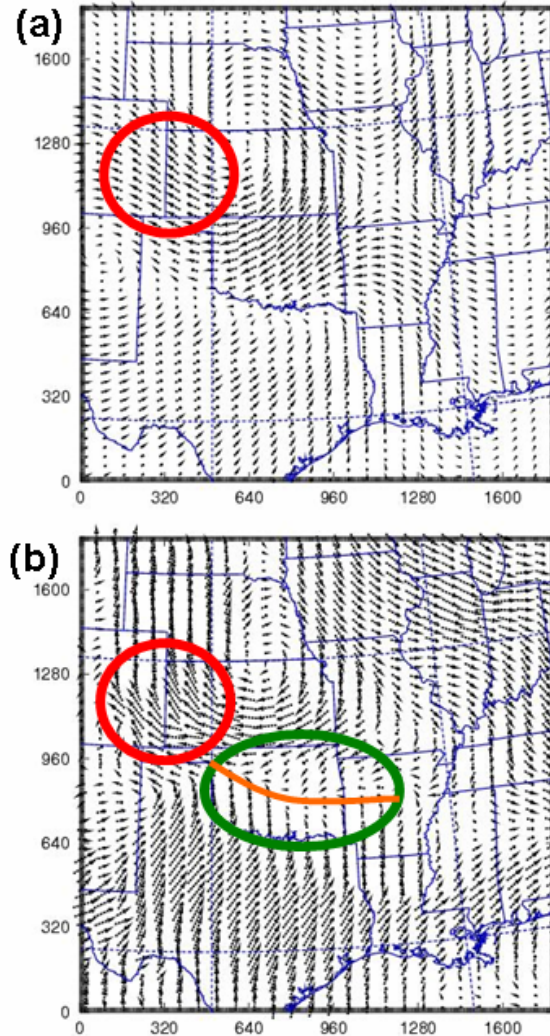


**Fig. 3.** The GSI analyzed vector wind increment field (a) and full vector wind field (b) using default decorrelation length of background error.

*b. Impact of background error decorrelation length*

In the first set of experiments, all observations from 5 radars are superobbed to a regular grid with a 0.1 degree resolution in the horizontal and a 500 m resolution in the vertical. We first examine the impact of the horizontal decorrelation length on the analysis. The default decorrelation length of the background errors used in GSI is estimated using the NMC method (Wu et al. 2002 and Wu 2005). The decorrelation length can be stretched by a stretching factor  $\lambda$ . In our experiments,  $\lambda$  is set to the default value of 1 in the control experiment and then to 0.25 in a sensitivity experiment. GSI analyses are obtained with above  $\lambda$

values, respectively, using the same background from the WRF-NMM analysis shown earlier for 0900 UTC and the super-obbed radial velocity data.

The GSI analysis increment and the analyzed vector wind field with  $\lambda = 1$  are shown in Fig. 3. The analyzed increment (Fig. 3a) is very smooth and the observations are generally spread too far. Correspondingly, the analyzed wind vectors within closed red circle in Fig. 3b may not be correct and appear too large, which should be the result of inappropriate background error correlations as far as the radar data are concerned. The constraints in GSI also include one for modeling surface friction effect and it is parameterized as part of the background error and balance constraints. The balanced part of temperature, surface pressure and potential function are proportional to the increment of stream function, and the coupling parameters are estimated through regression using the differences between 48 and 24 hr forecasts verifying at the same time, i.e., the NMC method. These constraints are designed for large scale flows. For radar observations that represent convective scale flows, these relations may not be appropriate.

It is encouraging to see that the location of wind shift line in Fig. 3b is reasonable when radar data are included compared with that without using radar data in Fig. 2 and the dominant wind directions near the boundary of Oklahoma and Kansas becomes northeasterly. However, the convergence zone is too broad-over 200 km near the center of Oklahoma and very weak along the shift line.

It is clear that the analysis with  $\lambda = 1$  is too smooth, a sensitivity experiment is therefore conducted with a reduced value of  $\lambda$ , at 0.25, which reduces the horizontal correlation length by a factor of 4. The GSI analyzed vector wind field and the analysis increment are shown in Fig. 4a and Fig. 4b, respectively. In comparison with the field in Fig. 3a, the wind shift line is now well-defined (Fig. 4a). In the analyzed wind field (Fig. 4b), much stronger and narrower convergence line is now found along the wind shift line and the strong winds inside red circles are reduced from those in the previous case.

These two experiments suggest that the default decorrelation length is too large for assimilating superobbed radar velocity. The radial velocity observational increments are spread too far and most of the convective-scale structures are filtered out. However, the assimilation is still very useful for capturing the convergence and wind shift line. After the analysis, the location of the wind shift line and the wind directions are both more realistic. When the decorrelation length is decreased to a more appropriate value, the convergence zone becomes narrower and the convergence becomes strong. The overall wind

structure becomes much more realistic and corresponds better with the precipitation system along the line.

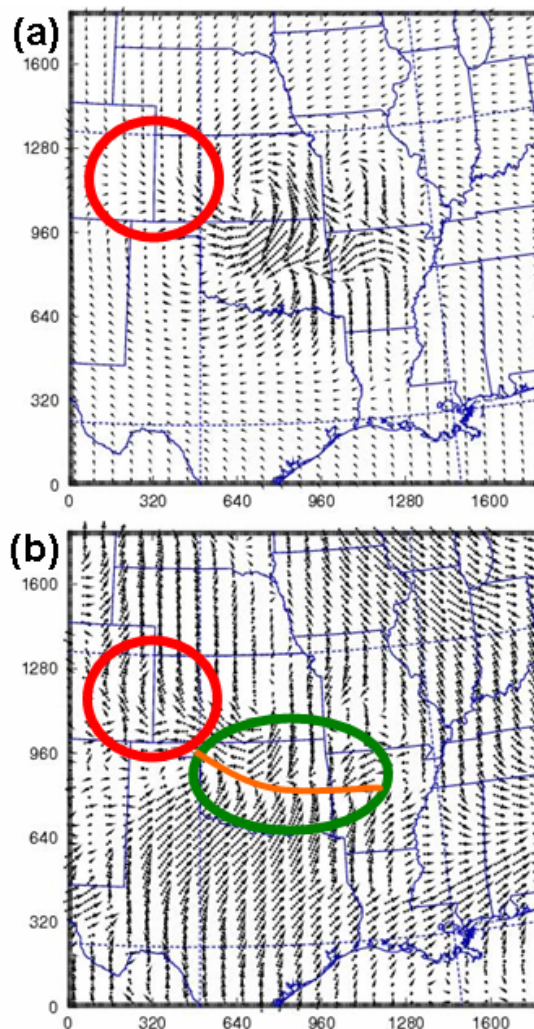


**Fig. 4.** Same as Fig. 2 but with a decorrelation length of 0.25, a quarter of the default value.

#### c. Impact of super-ob grid resolution

The resolution of superobbs, in terms of the grid spacing used by the superobbing technique, is another factor that impacts the radial velocity assimilation. When the super-ob grid resolution decreases, super-obbed radial velocity represents the average of radial velocities within a larger domain, therefore, the represented fields is smoother and small-scale features is missing. When super-ob grid resolution increases, more detailed structure can be retained but the cost of analysis increases. Finding an optimal super-ob size that balances between cost and analysis quality is necessary.

The impact of the super-ob grid resolution on the analysis is examined in this subsection. In this set of experiments, the vertical resolution is fixed at 500 m and the horizontal resolution is set to 0.05, 0.1, 0.25 and 0.5 degree, correspondingly. Only results from two experiments that use super-ob horizontal resolutions of 0.05° and 0.5°, respectively, are presented here. Same as the above experiments, the super-obbed radial velocities are formed from the 5 radars. GSI analyses are then performed using  $\lambda=0.25$  and the same background as used earlier.

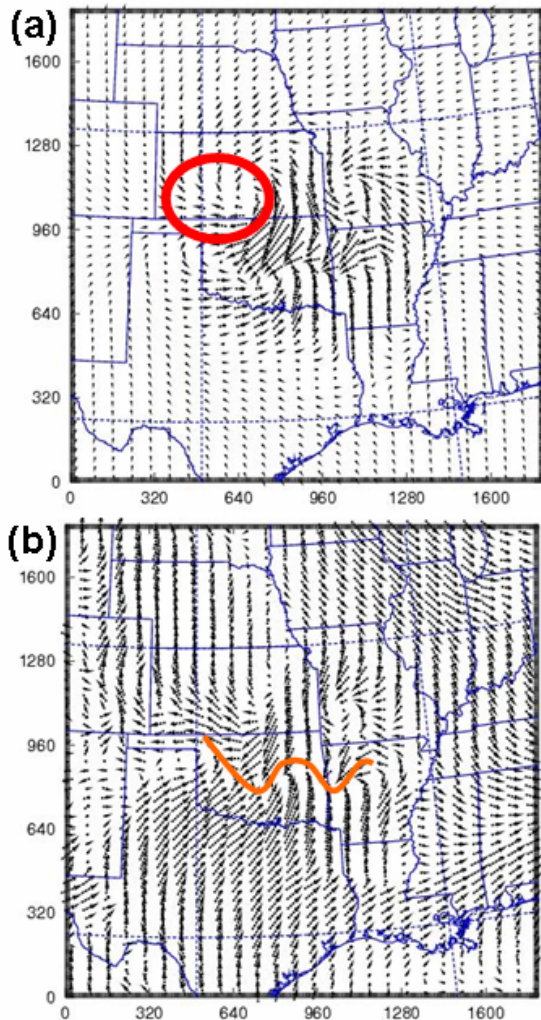


**Fig. 5.** Same as Fig. 2 but for a super-ob resolution of 0.05° in the horizontal.

The GSI analysis with the 0.05° horizontal super-obbing resolution is shown in Fig. 5. As can be seen from Fig. 5a, the winds within the closed red circle are weaker than those in Fig. 4a. Because the super-ob grid resolution is high in this experiment, the number of super-obbed radial wind observations is 4 times that of observations analyzed in the previous experiments.

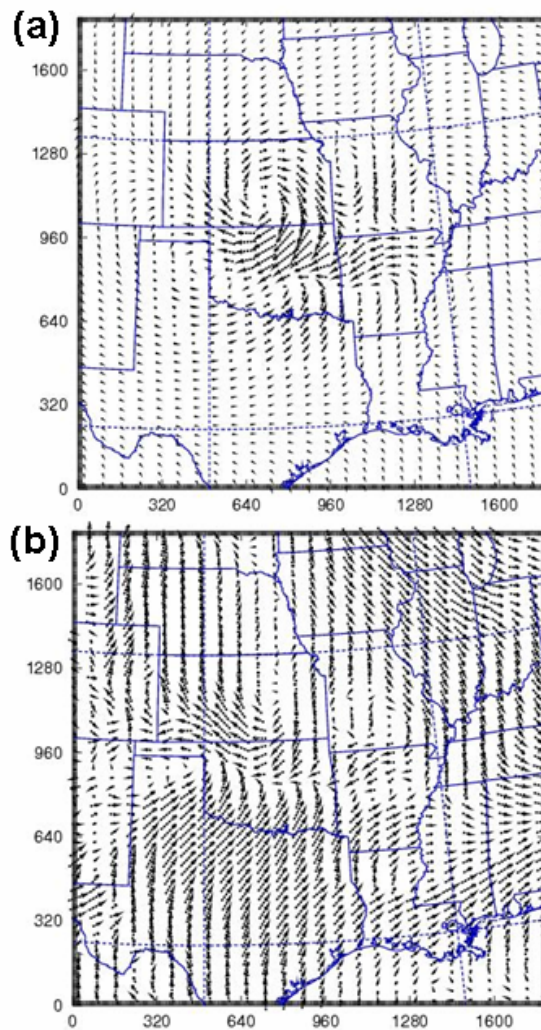


**Fig. 6.** Same as Fig. 2 but for a super-ob resolution of 0.5° in the horizontal.

When the number of the observations increases, the relative influence of the background constraint decreases, so are the influences of the built-in balance constraints. This explains why the winds in red circle are weaker, and closer to the radar observations. Comparing Fig. 5b with Fig. 1b the wind shift line in the GSI analysis matches the one indicated by the radar observations very well. In particular, the wind shift line curves bends towards the north at both ends, which agrees with the observations. This detailed structure is not clearly revealed, however, when the super-ob grid resolution is low. The GSI analysis with a horizontal superob resolution of 0.5° is shown in Fig. 6. As can be seen from Fig. 6a, the analysis increment field is smoother than that in Fig. 3a, because the super-obbed radial velocity data now represent the means of larger regions. Some small-scale information is therefore

missing in the analysis. The convergence of the analyzed field in Fig. 6a is clearly weaker than that seeing in Fig. 4a and 5a.

#### 4. Impact of radar radial wind on 6 hour forecast

The impact of radar radial wind on WRF-NMM short-term forecast is further examined using May 23 case. A horizontal resolution of 8 km was used over operational WRF-NMM central domain. Other parameter setting is the same as NCEP operational WRF-NMM. 6 hour forecasts starting from GSI analysis at 0600 UTC were performed. Note forecast starting from 0600 UTC is because the concerned system was under developing strategy and it became mature at 0900 UTC. Forecast starting from system developing strategy is easier to examine the impact of wind field. GSI analyzed fields without assimilating radial wind were used as background to further analyze radar radial winds. Similar to the experiments in previous section, the radial wind analysis at 0600 UTC was performed with different decorrelation length and super-ob grid resolution. Again, the analysis results showed that reducing decorrelation length and increasing super-ob grid resolution can improve GSI-analyzed wind fields at 0600 UTC also. The impact of decorrelation length and super-ob grid resolution on forecast was further examined by comparing forecast composite reflectivity and observed one.

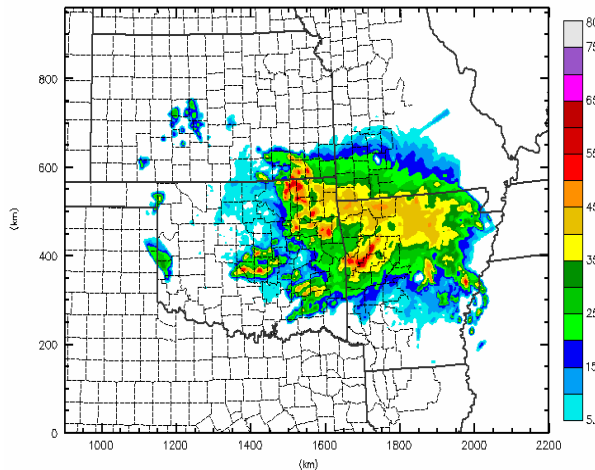


**Fig. 7.** Composite radar reflectivity at 1100 UTC.

It is found that the forecast system is about 1-h hour slower than the radar observation. The observed composite reflectivity at 1100 UTC is shown in Fig. 7. There are two large cells in the system in Fig. 7. The center of the first cell is near Oklahoma and Kansas boundary and the second one near Oklahoma and Arkansas boundary. They are well-separated. In the first experiment, the GSI-analyzed fields at 0600 UTC

using radar wind with default decorrelation length and 0.5 degree super-ob grid resolution were used to initiate WRF-NMM. The 6-h forecast composite reflectivity valid at 1200 UTC is shown in Fig. 8a. In the second experiment, the decorrelation length is set as a quarter of default one and super-ob grid resolution is set to 0.1°. The 6-h forecast composite reflectivity is shown in Fig. 8b. It is clear that composite reflectivity in Fig. 8b matches the match the observation in Fig. 8a better than that in Fig. 8a. Therefore, using reduced decorrelation length and high resolution super-ob in GSI radar wind analysis can further improve WRF-NMM forecast.

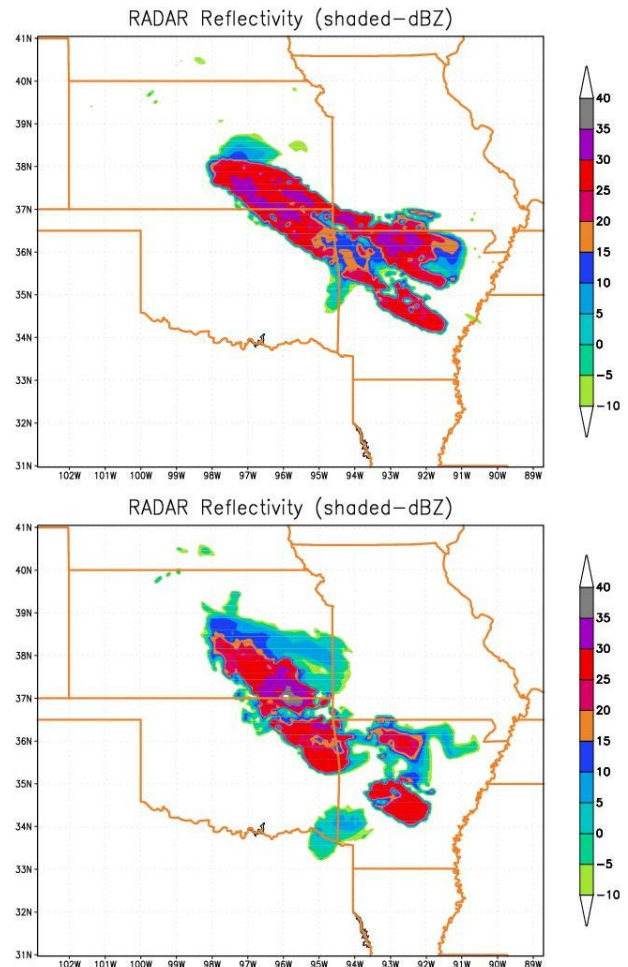


**Fig. 8.** 6-h forecast Composite radar reflectivity valid at 1200 UTC with default decorrelation length and 0.5° super-ob grid resolution (a) and with reduced decorrelation length (a quarter of default one) and 0.1° super-ob grid resolution (b)

## 5. Summary and conclusions

During a month visiting in EMC/NCEP and following-up one year, Shun Liu has integrated NSSL radar velocity QC package into NCEP real-time radar data flow and modified and improved the efficiency of QC package based on NCEP operational needs. The impacts of radar radial wind on GSI analysis and WRF-NMM forecast were examined.

The NCEP GSI 3DVAR analysis is used to analyze super-obbed radial velocity data from 5 WSR-88D radars for a mesoscale convective system that occurred on 23 May 2005 in the Kansas-Oklahoma boundary. The background the experimental is real time analysis of GSI on an 8 km WRF-NMM grid. In a sense, this presents a multi-pass analysis procedure in which data used in the current experimental system are analyzed in the first pass while radar data are analyzed in the second pass.

The impacts of the error decorrelation length of the background and the radar data super-obbing size or resolution on the quality of analysis is examined. The results show the default decorrelation length is too large for the analysis of radar data, which typically contain many convective-scale structures. This causes an unreasonably smooth analysis, with grid points far away from the radar observations being incorrectly influenced by the data. The strong smoothing causes the loss of convective scale structures in the analysis and results in a too weak convergence line, even though the radar data still show beneficial effects in such a case. As the decorrelation length decreases, the convergence near the wind shift line becomes stronger and the overall wind analysis is significantly improved.

In addition, given the fixed and relatively small, decorrelation length, increasing super-ob grid resolution further improves the analysis. More detailed structures are obtained. On the contrary, decreasing the super-ob grid resolution results in the loss of the small-scale details contained in the radar observations.

The impact of the radar wind on WRF-NMM forecast is also examined. When reduced decorrelation length and high resolution super-ob are used in radar data analysis via GSI, the short-term forecast composite reflectivity can be improved.

The raw radar observations have high resolutions in both space and time, and often contain much small-scale information in the presence of precipitation. Such small-scale information obviously should not be spread too far in space and the default decorrelation length derived for large-scale analysis based on, e.g. the NMC method, is apparently not suitable for radar data assimilation. Estimation of suitable decorrelation length using high-resolution data sets and the application of anisotropic background error covariance are desirable and planned.

## 6. Impact improvements in operational forecasting

- a. Shun Liu' visiting in EMC/NCEP obviously accelerated integrating NSSL radial velocity QC package into real-time radar data flow in NCEP.
- b. NCEP is very interested in testing result of impact of radar radial wind on GSI analysis and WRF-NMM forecast. More tests of the impact of background error dencorrelation length and super-ob resolution on GSI analysis and WRF-NMM forecast is under investigation in operational environment in EMC/NCEP.

## 7. List of papers from the project

Liu, S., M. Xue, J. Gao, and D. Parrish, 2005: Analysis and impact of super-obbed Doppler radial velocity in the NCEP grid-point statistical interpolation (GSI) analysis system. Extended abstract, *17th Conf. Num. Wea. Pred.*, Washington DC, 13A. 4.

Liu, S., M. Xue, J. Gao, and D. Parrish, 2006: Impact of background error covariance and superobbing scales on the analysis of Doppler radial velocity within GSI and on WRF-NMM forecast. *Mon. Wea. Rev.*, Under preparation.

*Acknowledgments.* This work was mainly supported by DOT-FAA grant via DOC-NOAA NA17RJ1227. M. Xue and J. Gao were also supported by NSF grants ATM-0129892 and ATM-0331756. M. Xue was further supported by NSF ATM-0331594 and EEC-0313747. Thanks Drs. Stephen Lord, Geoff DiMego, David Parrish, Wan-shu Wu, Matthew Pyle, Russ Treadon and Krishna Kumur for their help during Shun Liu's visiting in NCEP. Thanks Dr. Jidong Gao for discussion about radar wind assimilation. Thanks Drs. Qin Xu and Pengfei Zhang for their help and discussion during integrating NSSL radar radial velocity QC into NCEP real-time radar data flow.

## References

Gong, J., L. Wang, and Q. Xu, 2003: A Three-Step Dealiasing Method for Doppler Velocity Data Quality Control. *Journal of Atmospheric and Oceanic Technology*, 20, 1738-1748.

Liu, S., P. Zhang, L. Wang, J. Gong, and Q. Xu, 2003: Problems and solutions in real-time Doppler wind retrievals. Preprints, *31th Conference on Radar*

- Meteorology*, 6–12 August 2003, Seattle, Washington, Amer. Meteor. Soc., 308-309.
- Liu, S., M. Xue, J. Gao, and D. Parrish, 2005: Analysis and impact of super-obbed Doppler radial velocity in the NCEP grid-point statistical interpolation (GSI) analysis system. Extended abstract, *17th Conf. Num. Wea. Pred.*, Washington DC, 13A. 4.
- Liu, S., Q. Xu, and P. Zhang, 2005: Identifying Doppler Velocity Contamination Caused by Migrating Birds Part II: Bayes Identification and Probability Tests. *J. Atmos. Oceanic Technol.* **22**, 1114-1121.
- Parrish, D. F. and J. C. Derber, 1992: The National Meteorological Center's spectral statistical-interpolation analysis system. *Mon. Wea. Rev.*, **120**, 1747-1763.
- Parrish, D. F. 2005: Assimilation strategy for level 2 radar winds. *Presentation, 1<sup>st</sup> GSI User Orientation*. Camp spring, MD [available online at [http://wwwt.emc.ncep.noaa.gov/gmb/treadon/gsi/documents/presentations/1<sup>st</sup>\\_gsi\\_orientation](http://wwwt.emc.ncep.noaa.gov/gmb/treadon/gsi/documents/presentations/1<sup>st</sup>_gsi_orientation)].
- Purser, R. J., D. Parrish and M. Masutani, 2000: Meteorological observational data compression; an alternative to conventional "super-obbing". Office Note 430, National Centers for Environmental Prediction, Camp spring, MD [available online at <http://wwwt.emc.ncep.noaa.gov/officenotes/FullT OC.html#2000>]
- Purser, R. J., W.-S. Wu, D. F. Parrish, and N. M. Roberts, 2003a: Numerical aspects of the application of recursive filters to variational statistical analysis. Part I: Spatially homogeneous and isotropic Gaussian covariances. *Monthly Weather Review*, **131**, 1524-1535.
- , 2003b: Numerical aspects of the application of recursive filters to variational statistical analysis. Part II: Spatially inhomogeneous and anisotropic general covariances. *Monthly Weather Review*, **131**, 1536-1548.
- Wu, W.-S., R. J. Purser, and D. F. Parrish, 2002: Three-dimensional variational analysis with spatially inhomogeneous covariances. *Mon. Wea. Rev.*, **130**, 2905-2916.
- Wu, W.-S 2005: Background error and their estimation. *Presentation, 1<sup>st</sup> GSI User Orientation*. Camp spring, MD [available online at [http://wwwt.emc.ncep.noaa.gov/gmb/treadon/gsi/documents/presentations/1<sup>st</sup>\\_gsi\\_orientation](http://wwwt.emc.ncep.noaa.gov/gmb/treadon/gsi/documents/presentations/1<sup>st</sup>_gsi_orientation)].
- Xu, Q., L. Wang, P. Zhang, S. Liu, Q. Zhao, K. Sashegyi and J. Nachamkin, 2004: Progress in radar data quality control and assimilation. Preprints, *Sixth International Symposium on Hydrological Applications of Weather Radar*, 2-4 February 2004, Melbourne, Australia.
- Zhang, P., S. Liu and Q. Xu, 2005: Identifying Doppler velocity contamination caused by migrating birds Part I: feature extraction and quantification. *J. Atmos. Oceanic Technol.* **22**, 1105-1113.